NMR Investigations into the *Vase-Kite* Conformational Switching of Resorcin[4]arene Cavitands

by **Vladimir A. Azov**, **Bernhard Jaun**, and **François Diederich***

Laboratorium für Organische Chemie, ETH-Hönggerberg, CH-8093 Zürich
(e-mail: diederich@org.chem.ethz.ch)

Dedicated to Professor *K. N. Houk* at the occasion of his 60th birthday

We report the detailed investigation of temperature- and pH-triggered conformational switching of resorcin[4]arene cavitands **1**–**10** (*Figs. 1*, *8*, and *9*). Depending on the experimental conditions, these macrocycles adopt a *vase* conformation, featuring a deep cavity for potential guest inclusion, or two *kite* conformations (*kite 1* and *kite 2*) with flat, extended surfaces (*Schemes 1* and *2*). The thermodynamic and kinetic parameters for the interconversion between these structures were determined by variable-temperature NMR (VT-NMR) spectroscopy (*Figs. 2–7* and *10*, and *Tables 1* and *2*). It was discovered that *vase* → *kite* switching of cavitands is strongly solvent-dependent: it is controlled not only by solvent polarity but also by solvent size. Conformational interconversions similar to those of the parent structure **1** with four quinoxaline flaps are also observed when the octol base skeleton is differentially or incompletely bridged. Only octanitro derivative **2** was found to exist exclusively in the *kite* conformation under all experimental conditions. The detailed insight into the *vase* ⇌ *kite* conformational equilibrium gained in this investigation provides the basis for the design and construction of new, dynamic resorcin[4]arene cavitands that are switchable between bistable states featuring strongly different structures and functions.

1. Introduction. – Resorcin[4]arene cavitands with four quinoxaline bridges were originally introduced and studied by *Cram* and co-workers [1]. A particulary interesting feature of these systems is their ability to switch between two states, a *vase* conformation with a deep cavity well suitable for guest inclusion [2] (for a review on molecular encapsulation, see [3]) and a *kite* conformation featuring a large flat surface. This *vase* ⇌ *kite* equilibrium is controllable by both temperature- [1] or pH-variation [4], and resembles the movement of a molecular gripper. According to *Cram* and co-workers, the temperature dependence of the *vase* ⇌ *kite* equilibrium is caused by solvation effects: at low temperatures, solvation of the larger, solvent-exposed surface favors the *kite* conformer, whereas, at higher temperature, the entropic term $T\Delta S_{solv}$ for solvation of the larger *kite* surface becomes unfavorable, and the *vase* conformation predominates.

We are interested in the potential utilization of modified resorcin[4]arene cavitands as molecular grippers, capable of guest hosting and releasing on demand, in device construction at the single-molecule level. This objective requires a deeper mechanistic understanding of the *vase* ⇌ *kite* conformational equilibration. In this context, the discovery of pH-triggered *vase* → *kite* switching and the use of UV/VIS spectroscopy to monitor the interconversion had been reported earlier [4] (for a first scanning tunneling microscopy (STM) study, imaging the *vase* conformation at molecular

resolution, see [5]). Upon protonation, the cavitand changes from the *vase* into the *kite* conformation; such a change in molecular geometry can be attributed to protonation of the mildly basic quinoxaline N-atoms, resulting in electrostatic repulsion of the cationic cavitand walls in the *vase* form. The switching is reversed upon addition of base.

We have recently also reported the synthesis and solid-state structures of a series of novel, partially and asymmetrically bridged resorcin[4]arene cavitands, bearing dye labels and featuring a diversity of legs for surface immobilization [6]. Here, we present a detailed study of the temperature- and pH-triggered *vase* → *kite* conformational switching of these systems (for a preliminary report on parts of this work, see [7]). By variable-temperature NMR (VT-NMR) spectroscopy, we discovered a new interconversion between two *kite* forms (*kite 1* and *kite 2*; *Scheme 1*) and estimated the thermodynamic (ΔH and ΔS) and kinetic parameters ($\Delta H^{\neq}$ and $\Delta S^{\neq}$) for the equilibration between the three (*vase, kite 1*, and *kite 2*) conformational states. A solvent scan was performed to study the influence of the environment on the switching process.

Scheme 1. *Interconversions between* Vase, Kite 1, *and* Kite 2 *Conformations of Resorcin[4]arene Cavitands with Four Quinoxaline Flaps*

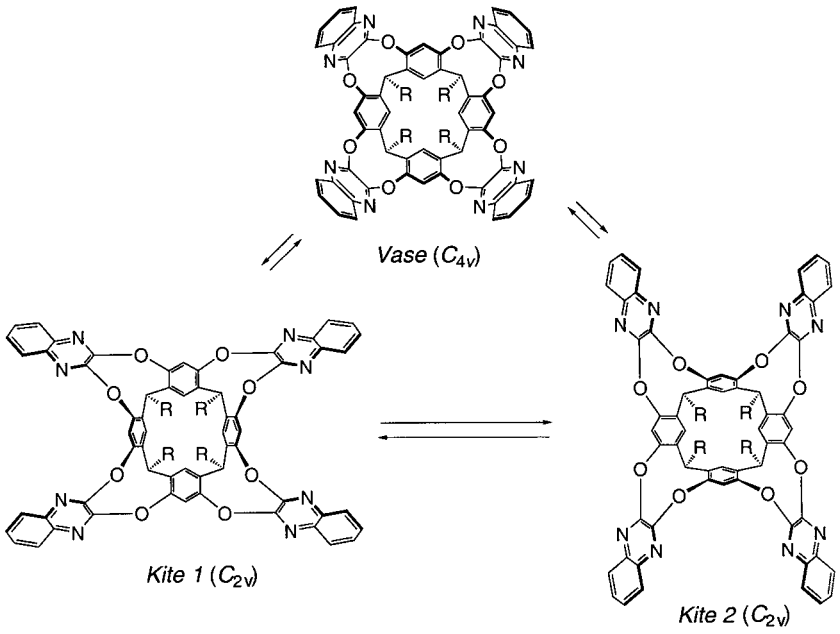

2. Results and Discussion. – 2.1. *VT-NMR Studies of* Vase ⇌ Kite *Conformational Equilibria*. The temperature- or acid-triggered *vase* → *kite* switching of resorcin[4]arene cavitands manifests itself by a change in the chemical shift of the methine H-atom H^a (*Fig. 1*) from $\delta \approx 5.5$ ppm in the *vase* to $\delta \approx 3.7$ ppm in the *kite* conformation. More-detailed VT-NMR studies with protonated cavitand **1** in acidic CD_2Cl_2 now led to the identification of a second, *kite 1* ⇌ *kite 2*, switching process (*Scheme 1*). This equili-

brium is fast on the NMR time scale at room temperature; thus, the ^{1}H-NMR spectrum of the protonated cavitand at 298 K is dynamically averaged and indicates an apparent fourfold symmetry of the *kite* conformer (*Fig. 2*). Upon cooling to *ca.* 250 K, the number of signals doubles, and the spectrum becomes consistent with the presence of two slowly interconverting *kite* conformers with C_{2v} symmetry. The same change in number of resonances was also observed by cooling a solution of neutral cavitand **1** in CD_2Cl_2 to 193 K, as a result of switching from the C_{4v}-symmetrical *vase* into two slowly exchanging C_{2v}-symmetrical *kite* forms (*Fig. 2*). These processes could also be monitored by ^{13}C-NMR spectroscopy, with a doubling of the resonances seen at low temperature for both neutral and protonated **1** (*Fig. 3*).

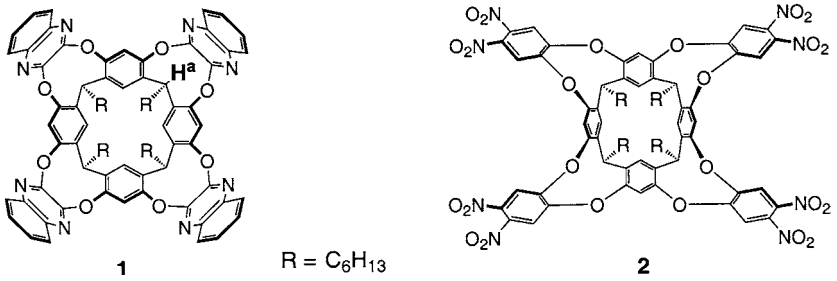

Fig. 1. *Cavitand structures* **1** *and* **2**

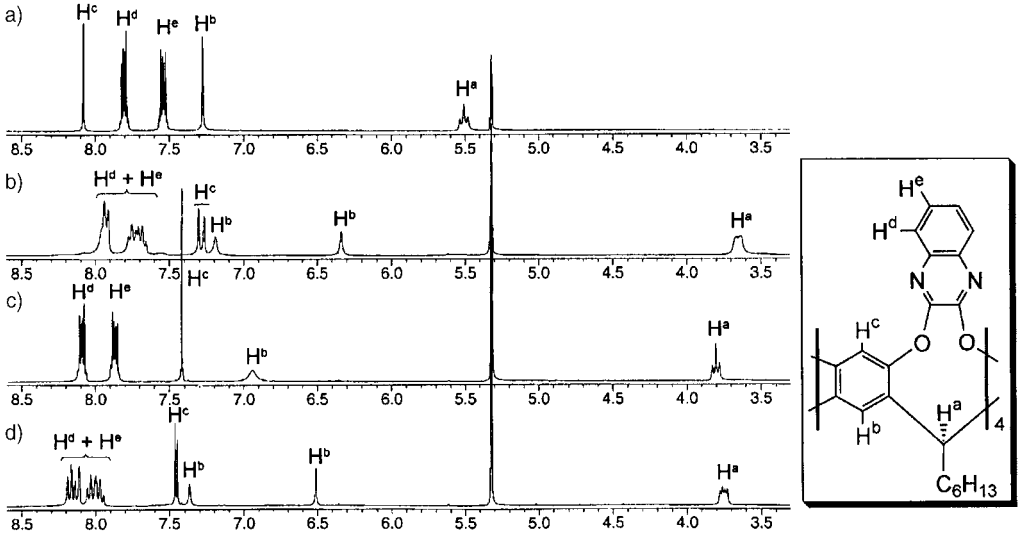

Fig. 2. *^{1}H-NMR Spectra of* **1** ($c = 1 \times 10^{-2}$ M, 300 MHz, CD_2Cl_2) *at* a) T = *295 K;* b) T = *193 K;* c) T = *308 K, 0.5*M *TFA added;* d) T = *243 K, 0.5*M *TFA added*. Only the aromatic region of the spectra is shown. TFA = CF_3COOH.

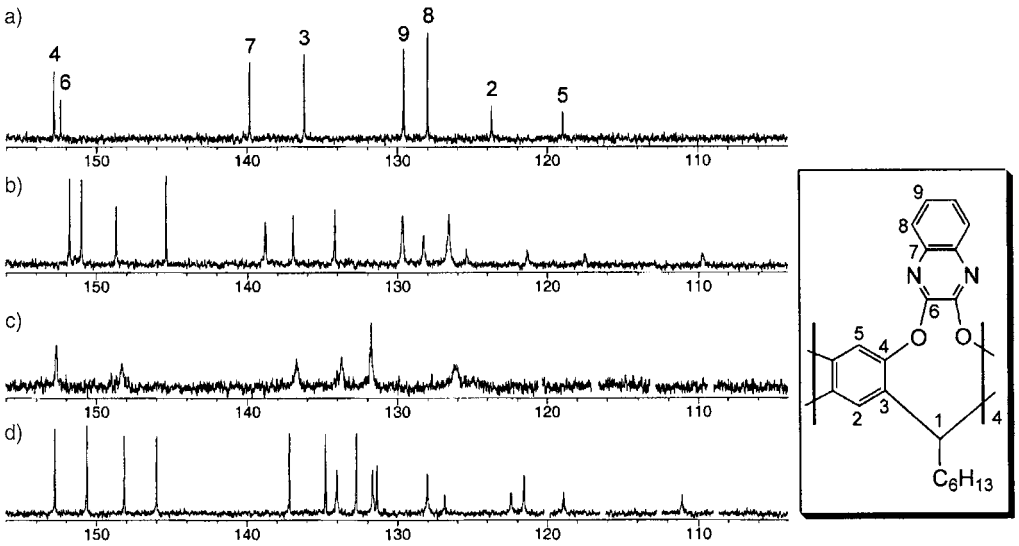

Fig. 3. *^{13}C-NMR Spectra of* **1** ($c = 1 \times 10^{-2}$ M, 300 MHz, CD_2Cl_2) *at* a) T = *295 K;* b) T = *193 K;* c) T = *308 K, 0.5*M *TFA;* d) T = *243 K, 0.5*M *TFA*. Only the aromatic region of the spectra is shown. TFA resonances are removed for clarity.

Recently, we showed by X-ray analysis that cavitand **2** (*Fig. 1*) prefers to adopt the *kite* conformation in the solid state [6]. VT-NMR Studies in $CDCl_3$, $(CD_3)_2CO$, and (D_8)THF confirmed that this is also the exclusive conformation in solution. Upon cooling from 350 to 240 K, the number of resonances doubled (*Fig. 4*), in agreement with the *kite 1* ⇌ *kite 2* equilibrium becoming slow on the NMR time scale. In the investigated temperature range, the methine H-atom resonance remained nearly constant at a position (*ca.* 4.3 ppm) characteristic for the *kite* structure, indicating that no switching to the *vase* conformation occurred (*Scheme 2*).

Scheme 2. *Conformational* Kite 1 ⇌ Kite 2 *Equilibration of Octanitrocavitand* **2**

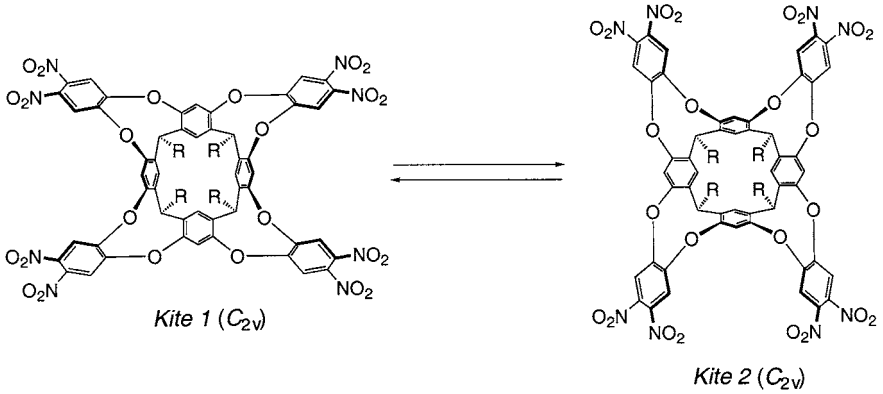

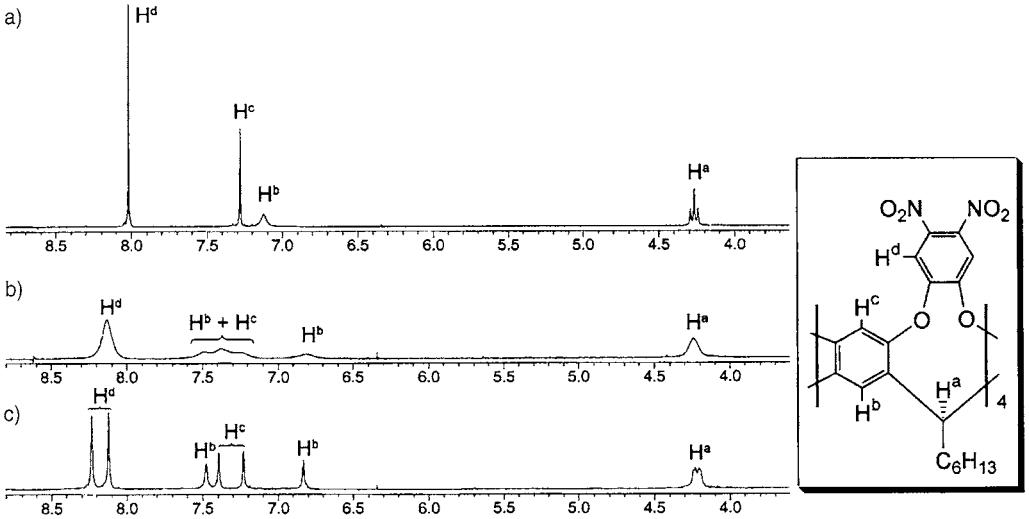

Fig. 4. *^{1}H-NMR Spectra of* **2** ($c = 2 \times 10^{-3}$ M, 300 MHz, $(CD_3)_2CO$) *at* a) T = *343 K* (fast exchange), b) T = *293 K* (near coalescence temperatures of H^b, H^c, and H^d), *and* c) T = *273 K* (slow exchange). Only the aromatic region of the spectra is shown.

By means of iterative lineshape calculations (see the *Exper. Part* for details), the activation parameters for the *kite 1* ⇌ *kite 2* equilibration of **2** in $CDCl_3$ and $(CD_3)_2CO$ were estimated by the method described by *Sandström* [8]. The resulting *Eyring* plot is shown in *Fig. 5*. In both solvents, the activation enthalpy $\Delta H^{\neq}$ was *ca.* 10–11 kcal · mol^{-1} and the activation entropy $\Delta S^{\neq} \approx -13$ cal · $mol^{-1} \cdot K^{-1}$ (*Table 1*).

Table 1. *Thermodynamic and Kinetic Parameters for Different Switching Modes of Cavitands* **1** *and* **2**

Cavitand	Conditions	Switching mode	ΔH [kcal · mol^{-1}]	ΔS [cal · $mol^{-1} \cdot K^{-1}$]	$\Delta H^{\neq}$ [kcal · mol^{-1}]	$\Delta S^{\neq}$ [cal · $mol^{-1} \cdot K^{-1}$]
2	$(CD_3)_2CO$	*kite 1* → *kite 2*	[a])	[a])	10.1 ± 1.5	−12.9 ± 3
2	$CDCl_3$	*kite 1* → *kite 2*	[a])	[a])	10.9 ± 1.5	−14.0 ± 3
1	CD_2Cl_2, 0.75M TFA	*kite 1* → *kite 2*	[a])	[a])	21.2 ± 1.5	26.6 ± 3
1	CD_2Cl_2, 0.43M TFA	*kite 1* → *kite 2*	[a])	[a])	17.4 ± 1.5	16.4± 3
1	CD_2Cl_2	*vase* → *kite*	−5.9 ± 0.5[b])	−25.8 ± 2[b])	3.8 ± 2	−33.2 ± 4
1	CD_2Cl_2	*kite* → *vase*	5.9 ± 0.5[b])	25.8 ± 2[b])	9.7 ± 2	−7.8 ± 4

[a]) Degenerate equilibrium. [b]) The values are averaged for three independent measurements.

The same method applied to the *kite 1* → *kite 2* switching of **1** in acidic CD_2Cl_2 (0.75M TFA) provided very different activation parameters (*Fig. 5*). Compared to **2**, the activation enthalpy (*ca.* 21 kcal · mol^{-1}) is much higher, and a large positive activation entropy (*ca.* 27 cal · $mol^{-1} \cdot K^{-1}$) was calculated. This could indicate that partial or full deprotonation, which is a high-activation-enthalpy process, is required in

the transition state of the conformational switching of protonated **1**. A deprotonated transition state structure would be less solvated than the protonated ground-state *kite* structure, which would explain the favorable activation entropy.

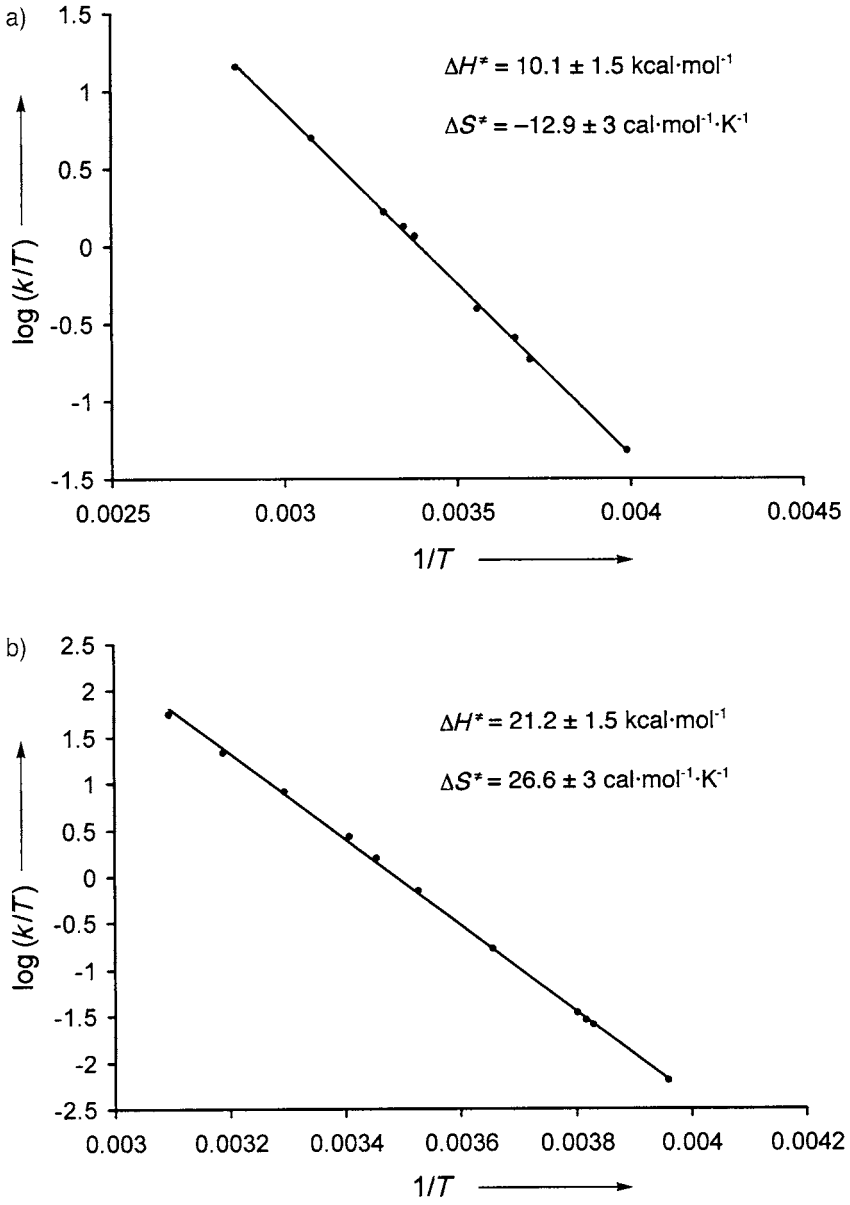

Fig. 5. Eyring *plot and activation parameters from calculated rate constants for the* kite 1 ⇌ kite 2 *equilibration* a) *of* **2** *in* $(CD_3)_2CO$ *and* b) *of protonated* **1** (1×10^{-2} M) *in* CD_2Cl_2 *containing 0.75* M *TFA*

In support of this explanation, the *kite 1* → *kite 2* switching occurred at a faster rate at lower acid concentration, when the cavitand may not be fully protonated. For example, coalescence for the H-atoms H^b occurred at 280 ± 1 K at 0.43M TFA and at 290 ± 1 K at 0.75M TFA. Lineshape fitting showed that the activation enthalpy decreased by *ca.* 3 kcal · mol^{-1}, whereas entropy decreased by *ca.* 10 cal · mol^{-1} · K^{-1} upon lowering the acid concentration (*Table 1*). Environmental polarity effects could, of course, also contribute to these changes in kinetics with changing TFA concentration; however, we have previously excluded such effects, at least for the *vase* ⇌ *kite* equilibration [4]. Lineshape fitting of VT-NMR spectra recorded at TFA concentrations of 0.2M or less did not yield interpretable results, likely due to the presence of small amounts of *vase* or partial-*vase* structures in the solution.

To simulate the *vase* ⇌ *kite* interconversion of neutral **1** by NMR lineshape fitting, it was necessary to determine the *vase*-to-*kite* ratios at different temperatures, *i.e.*, to know the equilibration enthalpy and entropy. The coalescence temperature for the *vase* → *kite* transition was determined to be 245 ± 1.5 K; below this temperature, individual methine peaks corresponding to the *vase* and *kite* conformers could be observed and integrated. To obtain reliable results, relatively concentrated samples of **1** ($c = 1 \times 10^{-2}$ M) were used, and 128–256 acquisitions were performed before *Fourier* transformation. Determination of the methine peak ratio at several temperatures in the 203–233 K range, followed by *Van't Hoff* analysis (*Fig. 6*), allowed us to calculate ΔH and ΔS for the *vase* → *kite* transition to be *ca.* -6 kcal · mol^{-1} and -26 cal · mol^{-1} · K^{-1}, respectively. Thus, *vase* → *kite* switching at low temperatures is an enthalpy-driven process, attributed to better solvation of the extended *kite* surface, as predicted earlier by *Cram* and co-workers [1].

The activation parameters were subsequently determined by iterative lineshape fitting of the NMR spectra, and the corresponding *Eyring* plot is shown in *Fig. 6*. Activation enthalpy and entropy were found to be *ca.* 4 kcal · mol^{-1} and -33 cal · mol^{-1} · K^{-1}, respectively, for the *vase* → *kite* transition of **1**, and *ca.* 10 kcal · mol^{-1} and -8 cal · mol^{-1} · K^{-1} for the *kite* → *vase* transition, respectively.

The similarity of the activation parameters for the *kite 1* → *kite 2* switching of **2** ($\Delta H^{\neq} = 10.1 \pm 1.5$ kcal · mol^{-1}, $\Delta S^{\neq} = -12.9 \pm 3$ cal · mol^{-1} · K^{-1} in $(CD_3)_2CO$) and the *kite* → *vase* transition of neutral **1** ($\Delta H^{\neq} = 9.7 \pm 2$ kcal · mol^{-1}, $\Delta S^{\neq} = -7.8 \pm 4$ cal · mol^{-1} · K^{-1} in CD_2Cl_2) is quite remarkable (*Table 1*). We interpret this as a strong indication that both processes proceed through similar, presumably partial-*vase*-like transition states. We hope to shed further light onto these switching pathways by spectroscopy on single molecules as well as by molecular-dynamics calculations.

2.2. *Solvent Dependence of the* Vase → Kite *Switching Process.* Since the temperature-triggered switching process is apparently driven by differential solvation of the quinoxaline flaps in the *vase* and *kite* conformation, we expected a significant influence of the solvent on the equilibration. Similarly, solvation effects should also influence the equilibration between neutral *vase* and protonated *kite* structures. To explore such effects by ^{1}H-NMR spectroscopy, we used a 5×10^{-3} M solution of cavitand **1** in various deuterated solvents. Temperature- and acid-triggered switching was readily observed in the apolar, non-aromatic solvents $CDCl_3$, $CDCl_3/CS_2$ 1:1, CD_2Cl_2, $C_2D_2Cl_4$, and CCl_4 (*Fig. 7*), with the acid-induced *vase* → *kite* switching being reversed upon addition of base (K_2CO_3). On the other hand, in $C_6D_5CD_3$, the neutral cavitand was frozen in the

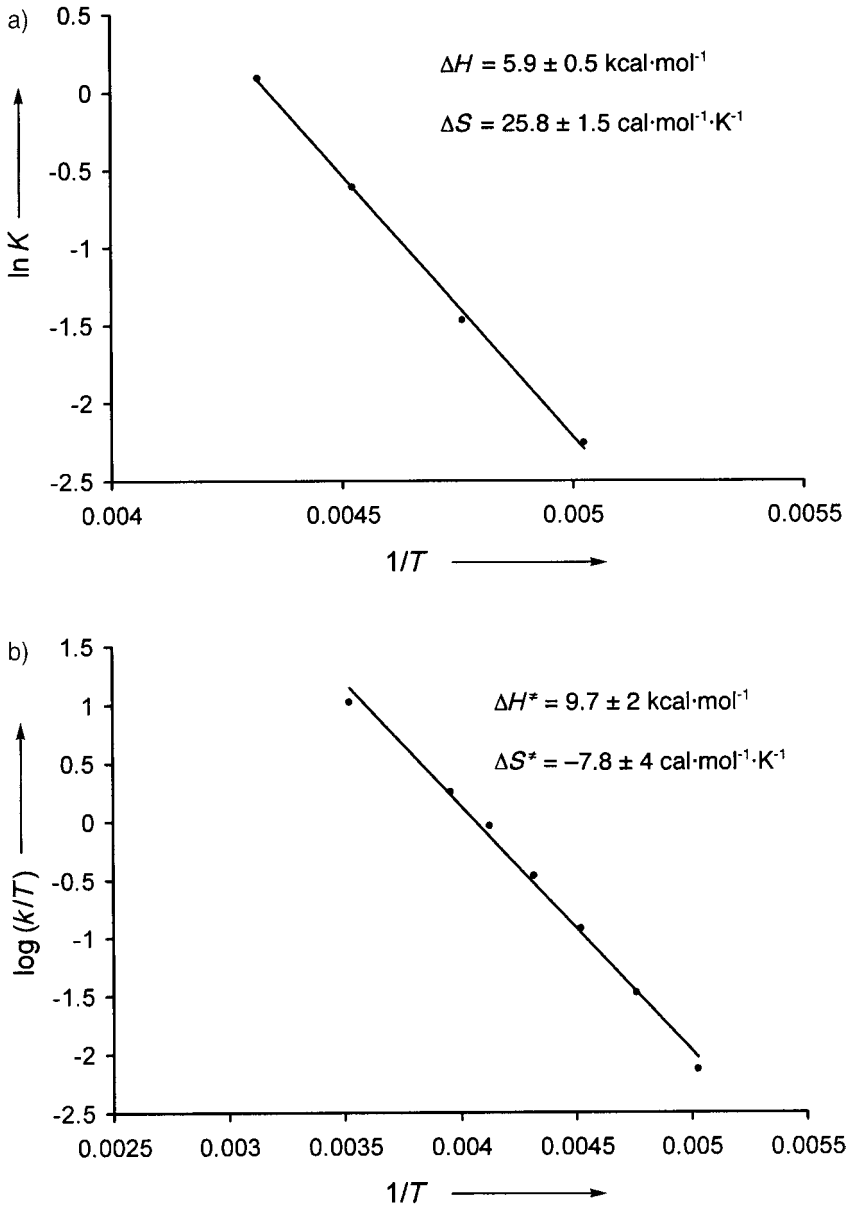

Fig. 6. a) Van't Hoff *plot and thermodynamic parameters for the* kite → vase *switching and* b) *Eyring plot and activation parameters from calculated rate constants for the* kite → vase *switching of neutral* **1** (1×10^{-2} M) *in* CD_2Cl_2

vase conformation over the entire temperature range between 313 and 193 K. However, addition of large quantities of CF_3COOH (TFA), ten times larger then required for complete switching in CD_2Cl_2 (*Fig. 7*), also induced the *vase* → *kite*

transition in the aromatic solvent. Similar results were obtained in deuterated benzene and fluorobenzene.

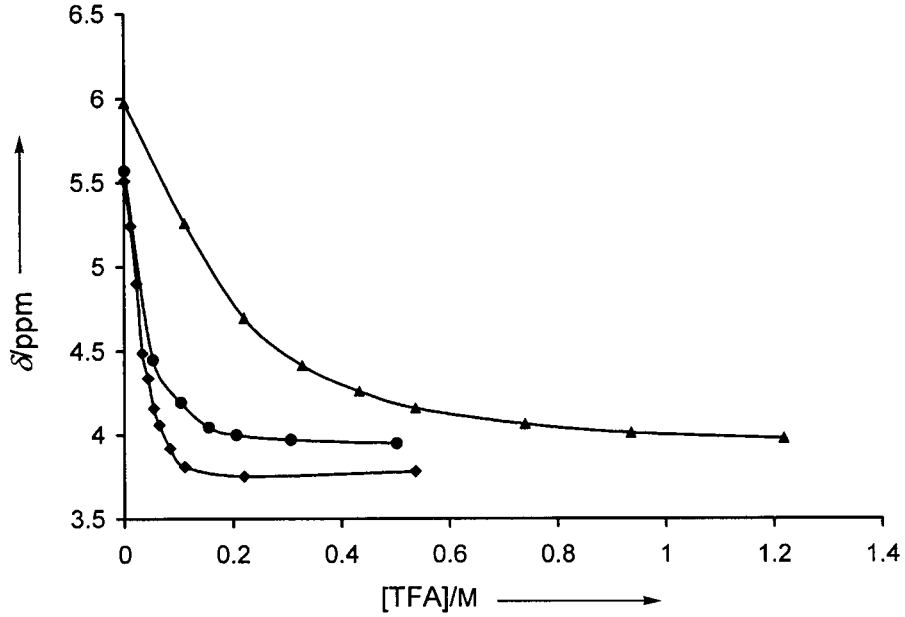

Fig. 7. *Change in chemical shift of the methine H-atom resonance of* **1** *upon addition of TFA to a solution of the cavitand in* CD_2Cl_2 (◆, similar in $CDCl_3$), *in* $C_6D_5CD_3$ (▲, similar in C_6D_6 and C_6D_5F), *and in* (D_{12})*-mesitylene* (●). $T = 295$ K, lines are eye guides.

Deuterated mesitylene ($C_6D_3(CD_3)_3$) appears to be a special case. Switching of **1** from the *vase* to the *kite* structure in this specific solvent required much smaller amounts of TFA than the equilibration in the other tested aromatic solvents. Similar to the experiment in CD_2Cl_2, complete *vase* → *kite* conversion was achieved at < 0.2M TFA (*Fig. 7*). In the absence of acid, all resonances remained broadened at 295 K, displaying resolved peaks corresponding to *vase* conformer at only *ca.* 370 K. Upon cooling to 253 K, the spectrum featured a pattern typical for the *kite* conformation, although peaks were broadened due to the high viscosity of mesitylene and, probably, to slowed but still occurring conformational interconversion. Addition of 2% (*v*/*v*) of deuterated benzene to the mesitylene solution at 295 K led to a resolved spectrum of the cavitand in the *vase* form, similar to that recorded in deuterated toluene or benzene. Upon standing, **1** slowly precipitated from mesitylene solution as a fine powder.

All these data imply that the *vase* ⇌ *kite* equilibrium is dependent not only on solvent polarity but also on solvent size [9]. Toluene, benzene, and fluorobenzene can nicely solvate the inner space of the *vase* conformation, thereby stabilizing this structure. On the other hand, mesitylene is too big to fit into the cavity, and hence only solvates efficiently the *kite* geometry. This in return facilitates the *vase* → *kite* conversion. These explanations are in agreement with the complexation ability of supramolecular capsules formed by resorcinarene cavitands as studied by *Rebek* and co-workers [3][10]. The width of the inner guest space in these capsules is similar to

that in the cavity of **1**. Correspondingly, benzene and toluene are well-encapsulated, whereas mesitylene is too large for complexation.

Finally, in the polar solvents (D_8)THF, (D_8)dioxane, and (D_6)acetone, no spectral changes upon temperature variation or TFA addition were observed, and the *vase* structure is clearly the preferred one. On the other hand, addition of CF_3SO_3H, a much stronger acid, to a solution of **1** in dioxane induces switching to the *kite* conformation, although this process is not reversible upon addition of base.

2.3. *Switching of Modified Cavitands.* The fully bridged cavitands **3**–**5** (*Fig. 8*) [6] all underwent both temperature- and pH-triggered conformational switching, although they show a higher preference for the *kite* conformation than the parent structure **1**. In variable-temperature runs, complete conversion of monosubstituted **3a** and **3b** into the *vase* form (all *multiplets* in the ^{1}H-NMR spectrum are resolved) occurred at 308 K in CD_2Cl_2, whereas the equilibration of disubstituted **4a** and **5a** was only completed at 333 K in $CDCl_3/CS_2$ (*Table 2*) or even at 363 K in CD_2Cl_2 (sealed tube). All structures **3**–**5** switched into the *kite* geometry at *ca.* 210 K; at that temperature, the NMR spectra displayed the presence of less than 5% of residual *vase* conformer. The higher preference for the *kite* conformation with increasing rim substitution (**1** < **3a**,**3b** < **4a**,**5a**) can be explained by both steric repulsion between the attached bulky groups and the favorable solvation of the enlargened surface in the open geometry. Cavitands **3**–**5** completely switched to the *kite* geometry upon addition of TFA; this process was reversible upon addition of base (K_2CO_3). The activation parameters for the *kite 1* ⇌ *kite 2* interconversion of **3b** were estimated to be similar to those of the parent cavitand **1**.

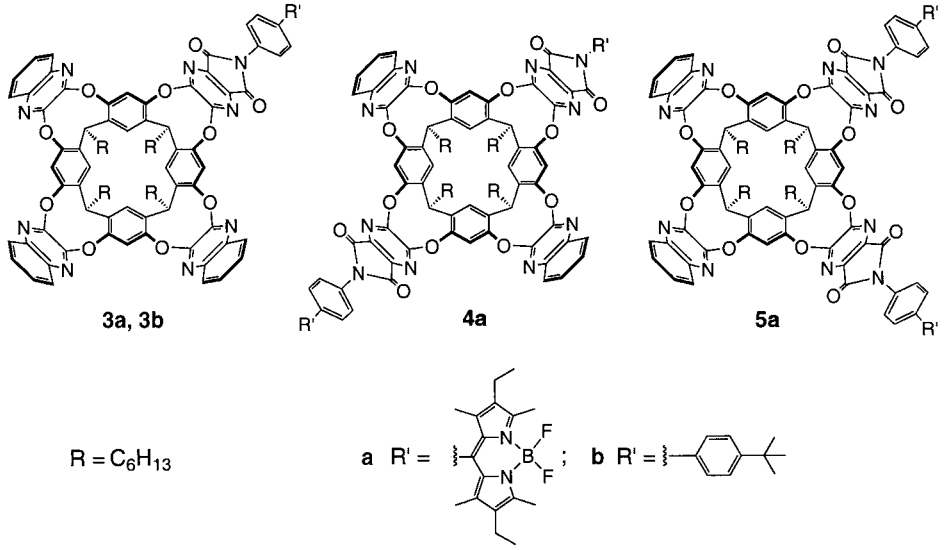

Fig. 8. *Differentially bridged cavitands*

Table 2. *^{1}H-NMR Investigation of the Temperature- or pH-Triggered* Vase–Kite *Isomerization, Monitoring the Methine Resonance of the Octol Bowl*

Cavitand	Solvent	δ_H [ppm]/T [K][a])	δ_H [ppm]/T [K][b])[c])	δ_H [ppm] at 0.5M TFA, 295 K[b])
1	CD_2Cl_2	5.51/293	3.65/203	3.76
3a	CD_2Cl_2	5.52 (3 H), 5.40/308	3.65/193	3.80
3b	CD_2Cl_2	5.48 (3 H), 5.35/308	3.67/193	3.80
4a	$CDCl_3/CS_2$ 1:1	5.56 (2 H), 5.37 (2 H)/333	3.71/193	3.89 (2 H), 3.83 (2 H)
5a	$CDCl_3/CS_2$ 1:1	5.56 (2 H), 5.35 (2 H)/333	3.71/193	3.97 (2 H), 3.91 (2 H)
6	CD_2Cl_2	5.61, 5.51 (2 H), 4.29/308	3.65 (3 H), 4.40/193	4.37, 3.96 (2 H), 3.85
7	CD_2Cl_2	5.39 (2 H), 4.36 (2 H)/293	–	4.43 (2 H), 3.74 (2 H)
8	CD_2Cl_2	5.52 (2 H), 4.22 (2 H)/293	–	4.35 (2 H), 3.79 (2 H)

[a]) Corresponds to predominant *vase* conformation. [b]) Corresponds to predominant *kite* conformation. [c]) *Multiplet* is not resolved.

Remarkably, even the partially bridged resorcin[4]arenes **6**, **7**, and **8** (*Fig. 9*) also underwent switching (*Table 2*). For diol **6**, low-temperature experiments revealed that the switching was not complete, *i.e.*, both *kite* and *vase* conformers were present in a *ca.* 1:1 ratio at 193 K (CD_2Cl_2). On the other hand, complete switching from *vase* to *kite* occurred upon addition of TFA, and the *kite 1* $\rightleftharpoons$ *kite 2* interconversion was observed as well. For tetraols **7** and **8**, low-temperature scans could not be performed since they started to precipitate from the solution below 273 K; addition of TFA at room temperature, on the other hand, led to complete transition from *vase* to *kite*.

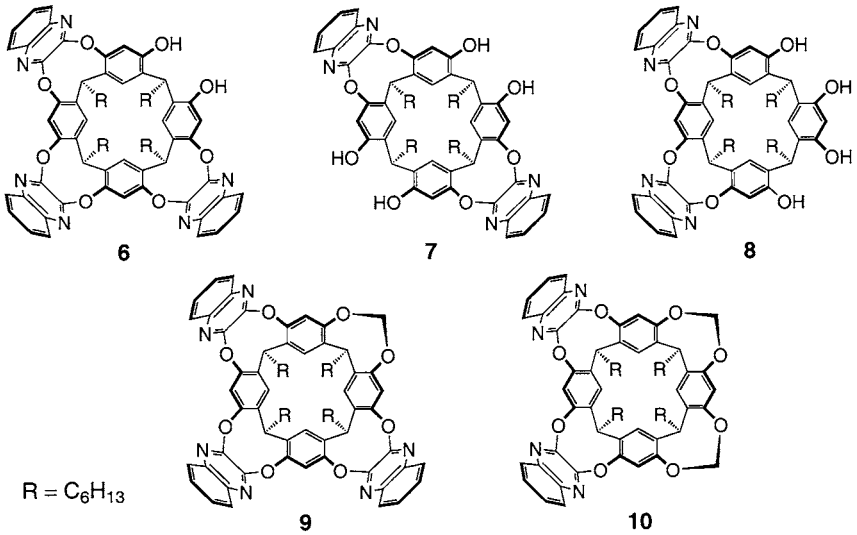

Fig. 9. *Partially bridged cavitands and cavitands with short aliphatic bridges*

Cavitands **9** and **10** were found in the *vase* conformation over the entire temperature range from 313 to 193 K in CD_2Cl_2. Addition of TFA at 295 K also did not induce switching to *kite*. Nevertheless, upon cooling the acidic solution to 243 K, the

methine H-atom peaks of both compounds shifted upfield by *ca.* 0.8 ppm, implying opening of the quinoxaline flaps to some extent.

3. Conclusions. – This detailed NMR investigation on a series of eleven resorcin[4]arene cavitands has provided many new insights into the conformational switching processes that are highly characteristic for this class of macrocycles. In addition to the previously reported temperature- or pH-triggered *vase* $\rightleftharpoons$ *kite* conformational equilibrium, a new equilibration process between two degenerate *kite* conformers was discovered. This process resembles equilibrations observed at much higher temperature for velcrands, bridged resorcin[4]arenes that exist only in the *kite* geometry [1c,d]. Among the macrocycles **1**–**10** addressed in this study, only octanitro derivative **2** is found exclusively in the *kite* form. The prediction by *Cram* and coworkers that *vase* → *kite* switching at low temperatures is an enthalpy-of-solvation-driven process, whereas the entropic term favors the reverse process at elevated temperature, was confirmed by *Van't Hoff* analysis. We take the similarity of the activation parameters, $\Delta H^{\neq}$ and $\Delta S^{\neq}$, obtained by NMR lineshape fitting, followed by *Eyring* plot analysis, for the degenerate *kite 1* → *kite 2* switching and the *kite* → *vase* transition as a strong indication that both processes proceed through similar, presumably partial-*vase*-like transition states, and we hope to further support this hypothesis in future molecular-dynamics simulations. A solvent scan revealed that switching is dependent not only on solvent polarity but also on solvent size. *Vase* → *kite* switching is best performed in chlorinated solvents such as $CHCl_3$, CH_2Cl_2, or $Cl_2CHCHCl_2$. This process becomes more difficult in aromatic solvents, such as benzene or toluene, that fit well into the cavity of the *vase* form and stabilize this geometry. Correspondingly, a larger aromatic solvent such as mesitylene facilitates the *vase* → *kite* transition since it is too bulky for occupying the *vase* cavity. Remarkably, *vase* → *kite* switching occurs even with partially bridged cavitands, with the protonation-triggered process generally being facilitated over the one induced by decreasing the solution temperature. The results of this investigation pave the way to the successful design of new types of dynamic molecular receptors that are switchable between bistable states, and greatly benefit our ongoing development of molecular grippers for use in construction at the single-molecule level.

Support by the *Swiss National Science Foundation*, *via* the *NFP* '*Supramolecular Functional Materials*' and the *NCCR* '*Nanoscience*', is gratefully acknowledged. We thank Mr. *Siefke Siefken* (ETH-Zürich) for help with NMR experiments.

Experimental Part

Determination of Thermodynamic and Kinetic Parameters for Conformational Switching, and Solvent Scan by NMR Spectroscopy. ^{1}H- and ^{13}C-NMR spectra were recorded with *Varian Mercury-300* and *Bruker AMX-500* spectrometers. Deuterated solvents were used as internal references: $CDCl_3$ (7.26 ppm for ^{1}H, 77.23 ppm for ^{13}C), CD_2Cl_2 (5.32 ppm for ^{1}H, 53.80 ppm for ^{13}C), $C_2D_2Cl_4$ (5.91 ppm for ^{1}H), C_6D_6 (7.15 ppm for ^{1}H), $C_6D_5CD_3$ (6.98 ppm for ^{1}H), C_6D_5F (7.15 ppm for ^{1}H), (D_{12})mesitylene (6.80 ppm for ^{1}H), $(CD_3)_2CO$ (2.05 ppm for ^{1}H), (D_8)THF (1.73 ppm for ^{1}H), (D_8)dioxane (3.53 ppm for ^{1}H). TMS was used as an internal reference in CCl_4. Low-temperature NMR was performed on a *Varian Mercury-300* spectrometer. The temp. was calibrated with 100% MeOH ($T \leq 313$ K) or $HOCH_2CH_2OH$ ($T \geq 313$ K) reference samples. Temp. regulation was stable within $\pm 0.5°$ between 363 and 243 K, and within $\pm 1.5°$ at lower temp. Peak assignments in the ^{13}C-NMR

spectra and of the aromatic H-atoms of **1** (*Fig. 2*) were accomplished on the basis of HMBC and HSQC experiments.

Fitting of the NMR spectra was performed with the *gNMR v3.6 for Macintosh* program (*Cherwell Scientific Publishing, Ltd.*, Oxford, UK). For the lineshape fitting of the *kite 1* ⇌ *kite 2* equilibrium of cavitands **1** and **2**, the H-atoms H^b and H^c (*Figs. 2* and *4*) were included in a two-site exchange model. For the lineshape fitting of the *vase* ⇌ *kite* equilibrium of **1**, H^a and two H-atoms of neighboring CH_2 groups (equivalent in the *vase* and non-equivalent in the *kite* conformation) were included into the two-site exchange model. An example of experimental and fitted spectra in the VT-NMR series is shown in *Fig. 10*.

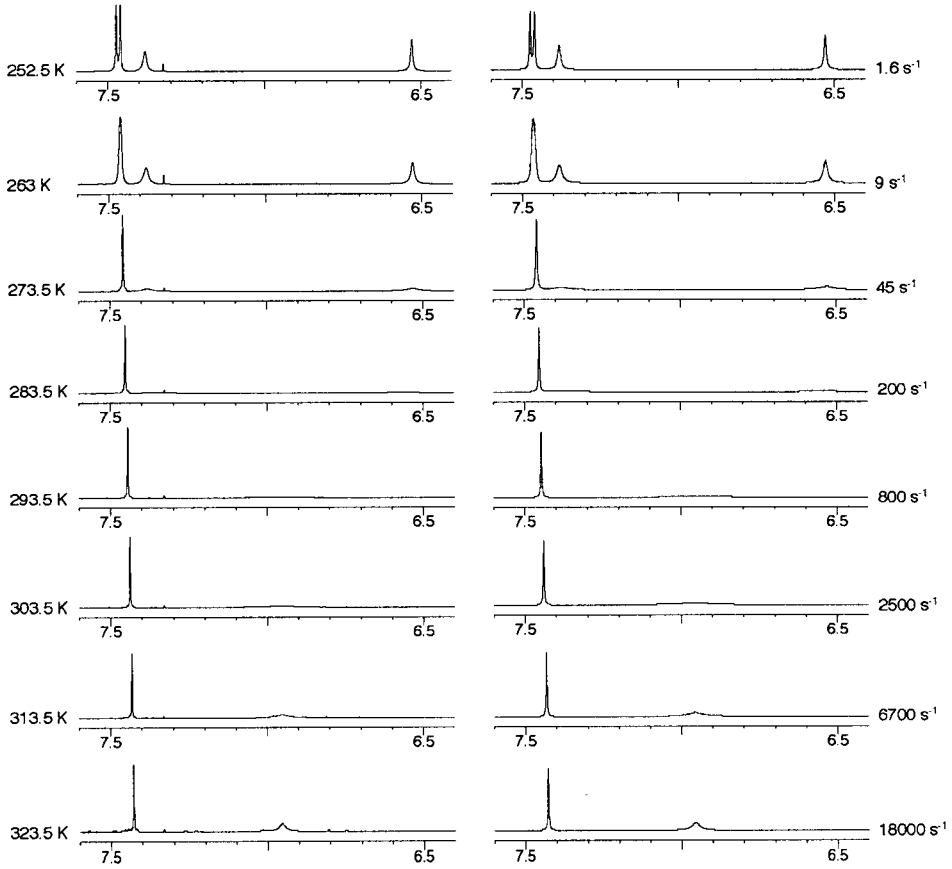

Fig. 10. *Comparison of experimental ^{1}H-NMR spectra* (left, 300 MHz, CD_2Cl_2, 0.75M TFA) *to fitted ones* (right) *of cavitand* **1** *at different temperatures.* The protons H^b and H^c were included in the model.

Determination of activation enthalpy and entropy was based on *Eqn. 1* [8]:

$$\log (k/T) = -\Delta H^{\neq}/aT + \Delta S^{\neq}/a + 10.319 \quad (1)$$

where k [Hz] is an exchange constant obtained from spectral fitting, T the temp. in K, and $a = 1.914 \cdot 10^{-2}$ for $\Delta H^{\neq}$ in kcal · mol^{-1} and $\Delta S^{\neq}/a$ in kcal · mol^{-1} · K^{-1}. According to *Eqn. 1*, a plot of log (k/T) *vs.* $1/T$ (*Eyring* plot) has a slope of ($-\Delta H^{\neq}/a$) and an intercept at $1/T = 0$ of ($\Delta S^{\neq}/a + 10.319$). *Eqn. 2* was used to calculate the free energy of activation at the temp. of coalescence of an equally populated two-site systems [8]:

$$\Delta G_c^{\neq} = aT[9.972 + \log(T/\delta\nu)] \quad (2)$$

where T is the temperature in K, $\delta\nu$ [Hz] the chemical shift between two coalescing resonances in the absence of exchange, and $a = 1.914 \cdot 10^{-2}$ for $G_c^{\neq}$ in kcal $\cdot$ mol^{-1}.

REFERENCES

[1] a) J. R. Moran, S. Karbach, D. J. Cram, *J. Am. Chem. Soc.* **1982**, *104*, 5826; b) J. R. Moran, J. L. Ericson, E. Dalcanale, J. A. Bryant, C. B. Knobler, D. J. Cram, *J. Am. Chem. Soc.* **1991**, *113*, 5707; c) D. J. Cram, H.-J. Choi, J. A. Bryant, C. B. Knobler, *J. Am. Chem. Soc.* **1992**, *114*, 7748; d) D. J. Cram, J. M Cram, 'Container Molecules and Their Guests', Royal Society of Chemistry, Cambridge, 1994, p. 107 – 130.

[2] a) M. Vincenti, E. Dalcanale, P. Soncini, G. Guglielmetti, *J. Am. Chem. Soc.* **1990**, *112*, 445; b) P. Soncini, S. Bonsignore, E. Dalcanale, F. Ugozzoli, *J. Org. Chem.* **1992**, *57*, 4608.

[3] F. Hof, S. L. Craig, C. Nuckolls, J. Rebek Jr., *Angew. Chem.* **2002**, *114*, 1556; *Angew. Chem., Int. Ed.* **2002**, *41*, 1488.

[4] P. J. Skinner, A. G. Cheetham, A. Beeby, V. Gramlich, F. Diederich, *Helv. Chim. Acta* **2001**, *84*, 2146.

[5] Y. Yamakoshi, R. R. Schlittler, J. K. Gimzewski, F. Diederich, *J. Mater. Chem.* **2001**, *11*, 2895.

[6] V. A. Azov, P. J. Skinner, Y. Yamakoshi, P. Seiler, V. Gramlich, F. Diederich, *Helv. Chim. Acta* **2003**, *86*, 3648.

[7] V. A. Azov, F. Diederich, Y. Lill, B. Hecht, *Helv. Chim. Acta* **2003**, *86*, 2149.

[8] J. Sandström, 'Dynamic NMR Spectroscopy', Academic Press, London, 1982, p. 93 – 123.

[9] K. T. Chapman, W. C. Still, *J. Am. Chem. Soc.* **1989**, *111*, 3075.

[10] T. Heinz, D. M. Rudkevich, J. Rebek Jr., *Nature* **1998**, *394*, 764; T. Heinz, D. M. Rudkevich, J. Rebek Jr., *Angew. Chem.* **1999**, *111*, 1206; *Angew. Chem., Int. Ed.* **1999**, *38*, 1136; S. K Körner, F. C. Tucci, D. M. Rudkevich, T. Heinz, J. Rebek Jr., *Chem.–Eur. J.* **2000**, *6*, 187; J. Chen, J. Rebek Jr., *Org. Lett.* **2002**, *4*, 327.

Received September 5, 2003